

Quantitative analysis of temporal variations on shoreline change pattern along Ganjam district, Odisha, east coast of India

Vipin Joseph Markose¹ · B. Rajan¹ · R. S. Kankara¹ · S. Chenthamil Selvan¹ · S. Dhanalakshmi¹

Received: 3 November 2015 / Accepted: 7 May 2016 / Published online: 21 May 2016
© Springer-Verlag Berlin Heidelberg 2016

Abstract This research work describes the shoreline change rate variations of Ganjam district of Odisha, east coast of India for the past 24 years. Seven shorelines were extracted from multidated satellite images, and shoreline change rate has been calculated by using digital shoreline analysis system. Long-term shoreline change rate (1990–2014) of the study area has been calculated using weighted linear regression method. Short-term changes have been computed for different time scales, i.e., 1990–1999, 1999–2006, 2006–2008, 2008–2013 and 2013–2014 using end point rate method. The results obtained from the study show that 71.65 % of Ganjam coast shows accretion pattern and 28.35 % of coast falls under erosion category. High erosion is mainly noticed in northern side of Gopalpur port which is mainly due to recent construction activities. Short-term results reveals that 2006–2008 period shows maximum erosion and 1999–2006 period exhibit maximum accretion in Ganjam coast. From short-term analysis, it is observed that shoreline in the study area shows cyclic nature of erosion and accretion pattern. The study reveals that tropical cyclones and human activities such as port development, construction of breakwaters and groins are the major factors responsible for shoreline erosion in the study area.

Keywords Erosion · Cyclone · Rushikulya river · DSAS · Weighted linear regression

Introduction

Rapidly eroding coastline is one of the major issues for many countries in the world. The exact causes of coastal erosion vary from place to place, and they depend on local oceanographic/climatic conditions. Because of this non-uniformity, it is necessary to study the individual or combination of factors which control the shoreline configuration. Li et al. (2014) have observed that apart from hydrodynamic processes, river sediment load is a major controlling factor for shoreline changes. Using long-term climatological data, many studies (e.g., Jimenez et al. 1997; Luecke et al. 1999; Malini and Rao 2004; Syvitski and Saito 2007) found positive correlation between shoreline change with rainfall and river discharge. The research work conducted in Jonian coast, Italy, shows that apart from reduction in river sediment discharge, anthropogenic activities such as sand mining, barrage construction, etc. are the major factors responsible for shoreline variations (Aiello et al. 2013). The study carried out in delta regions of the world such as Nile, Mekong, Indus, Huanghe, etc. found that dam construction across the rivers are the major causes for shoreline changes (Frihy and Dewidar 2003; Thanh et al. 2004; Giosan et al. 2006; Chu et al. 2006). Another factor which affects the shoreline variation is developmental activities such as harbor development, construction of groin, breakwater, etc. Kim et al. (2014) found that coastal erosion in Bongpyeong beach is mainly due to the expansion and construction of Jukbyeon harbor. Their results show that after construction of breakwaters significant morphological changes were occurred. Jayappa et al. (2003) have studied the impact of coastal structure on shoreline position of Mangalore coast. Coastal changes due to natural and anthropogenic activities have been studied by using various techniques such as

✉ R. S. Kankara
kankara@icmam.gov.in

¹ Integrated Coastal and Marine Area Management Project
Directorate (ICMAM-PD), NIOT Campus, Velachery,
Chennai 600100, India

remotely sensed data, beach profile analysis, and GPS surveys. All these methods have several advantages and limitations. Remotely sensed data products such as satellite images and aerial photographs are widely used for shoreline change studies. Satellite images are the most convenient method for shoreline demarcation because of its wide coverage and less expensiveness. Aerial photographs are also used for shoreline change analysis with high accuracy (Gonçalves et al. 2012; Ford 2013; Shtienberg et al. 2014).

Oceanographic parameters such as waves, currents, tides, and longshore drift are the major factors which control the shoreline configuration (Albert and Jorge 1998; Morton and Miller 2005). In some cases, extreme events such as storm surges and tsunamis are also causes for shoreline changes (Houser et al. 2008). Rapid shoreline changes will occur in a place where the longshore drift is interrupted by artificial structures. Bastos et al. (2012) have studied the impact of breakwater on morphological changes of Douro estuary sand spit of Portugal and found that significant changes have occurred after breakwater construction. Samsuddin and Suchindan (1987) have observed a direct relation between longshore current and erosion accretion rate in Kerala coast. Ramana Murthy et al. (2007) have studied shoreline evolution and sediment transport of Ennore port, Chennai, SE coast of India. They found that due to the interception of longshore drift by the breakwaters northern part of the port exhibits erosion while the southern part shows accretion. In India, many studies (e.g., Jayappa et al. 2003; Ranga Rao et al. 2009; Thiruvencatasamy and Girija 2014; Mohanty et al. 2015) have reported the longshore drift interception due to coastal structures which leads to erosion in one side and accretion in other side of the structures.

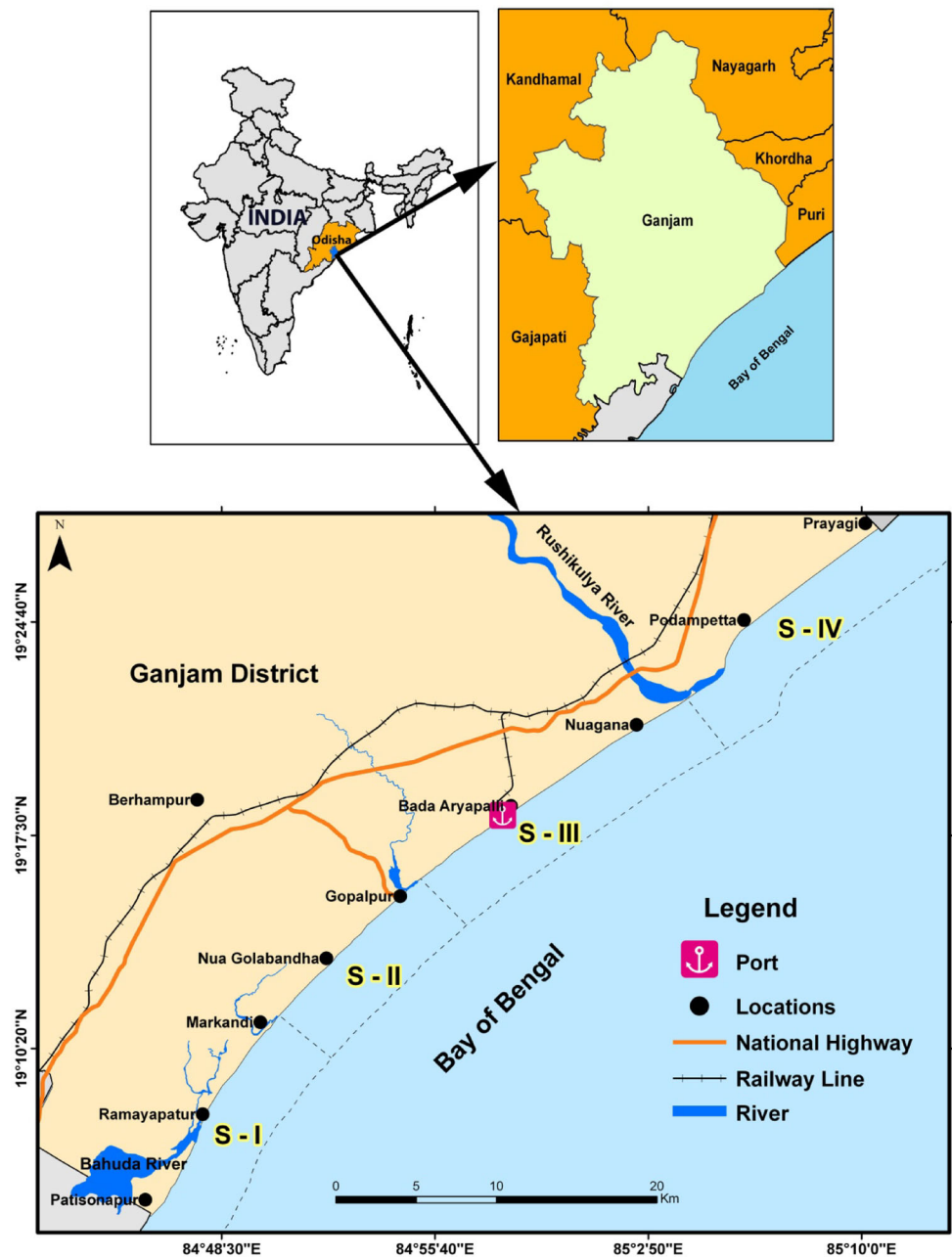
El Banna and Hereher (2009) have analyzed shoreline changes of north Sinai, Egypt, using satellite images. Maiti and Bhattacharya (2009) have applied statistics-based approach for long-term shoreline change analysis and prediction of future shoreline position of Balasore and Midnapur coast of Odisha and West Bengal. Sridhar et al. (2009) have estimated long-term shoreline oscillation of Cauvery delta using remote sensing and GIS techniques. Rao et al. (2010) have examined the relation between the shoreline change and sediment discharge. Their result shows decreasing sediment delivery and increasing erosion along the Krishna–Godavari delta front coast during past four decades. Using regularized single transect method, Anderson et al. (2015) have estimated long-term shoreline changes at Hawaii. Many statistical methods such as end point rate (EPR), linear regression rate (LRR), weighted linear regression (WLR), net shoreline movement (NSM) and least mean square (LMS) are widely used for shoreline change rate analysis (Dolan et al. 1991; Maiti and Bhattacharya 2009; Kuleli et al. 2011; Natesan et al. 2013;

Manca et al. 2013; Ozturk et al. 2015; Guneroglu 2015; Selvan et al. 2016). Zviely et al. (2009) have analyzed 200-year shoreline change rate of Haifa bay using different published maps. Hanamgond and Mitra (2007) have calculated the change detection of Karwar coast for 24 years (1989–2003). Mani Murali et al. (2009, 2015) have studied the erosion/accretion pattern of Puri and Kendrapara coast of Odisha using multidated satellite images. Natesan et al. (2013) have used conventional and modern techniques for estimation of shoreline changes along Vedaranyam coast, Tamil Nadu. Kaliraj et al. (2013, 2015) have studied the erosion and accretion pattern along southwest coast of Kanyakumari, Tamil Nadu, using remote sensing and GIS techniques. Recent study carried out by Kankara et al. (2014, 2015) classified the coast in different erosion/accretion (high, low, medium, etc.) classes to prepare shoreline change maps for Indian coast. Ozturk and Sesli (2015) have quantified the land loss/gain due to shoreline change of Kizilirmak delta using multidated satellite data. Recent shoreline change study of Indian coast shows that 45.5 % of the coast falls under erosion, 35.7 % shows accretion, and 18.8 % of the coast is more or less stable in nature (Rajawat et al. 2015). The objectives of this study are to estimate the temporal variation of shoreline change rate of Ganjam district, east coast of India for the past 24 years and examine the major factors which control the shoreline configuration. This was done by compiling the shoreline from multidated satellite images of different period from 1990 to 2014.

Study area

The coastline of Ganjam district is located in southern part of Odisha state, east coast of India and lies between 19° 07' N to 19° 46' N Latitude and 84° 76' E to 85° 17' E Longitude (Fig. 1). The district covers 61.64 km stretch of coastline starting from Patisonapur in south to Prayagi in north. The Ganjam coast is characterized by several geomorphic features like beach ridges, sand spits, and barrier spit. Physiographically, the district can be grouped into two divisions such as coastal plains in the east and hilly region in the west. The second largest mass nesting site of Olive Ridley sea turtles (*Lepidochelys olivacea*), i.e., Rushikulya rookery is located in the district. There are ~16 fish landing centers, and one major port, i.e., Gopalpur is found in the district. The beach sand in the Ganjam consists of economically important heavy minerals such as ilmenite, monazite, rutile, zircon, and garnet. Geologically, the coastal zone of Ganjam consists of Holocene beach sediment. The area is vulnerable for natural hazards such as cyclones, storm surges, flood, and coastal erosion.

Fig. 1 Map showing location and different sectors of Ganjam coast



The study area falls under tropical monsoon climatic zone with mean annual rainfall of ~1276 mm. Most of the rainfall events occurred during June to September which is considered as south west (SW) monsoon period. October to November is known as postmonsoon period with frequent occurrence of cyclonic storms with heavy rains. In summer season, the temperature will rise up to 40 °C and in winter it will be reduced up to 15 °C. The area falls under the microtidal area with a tidal range of <2 m. Mohanty et al. (2012) found that average spring and neap tidal ranges are 2.39 and 0.85 m, respectively, in Odisha coast. Sanil Kumar et al. (2006) have identified southwest and northeast

wind and wave regimes along east coast of India. Measured wave data off Gopalpur shows variation of 0.5 to 2.2 m in significant wave height (H_s) during June–September, 2–2.4 m during October–January, and 0.2–2.2 m during February–May (Chandramohan and Nayak 1994). The earlier reported maximum H_s off Gopalpur based on measured wave data was 2.4 m in 1990 (Chandramohan et al. 1993) and 3.3 m in 2008 (Mohanty et al. 2012). According to Mishra et al. (2011), high energy waves are generated during June–September (SW monsoon) and low to very low energy waves are occurred during March to May and December to February. Measured wave direction

off Gopalpur shows that $\sim 84\%$ of waves reach the coast between 135° and 180° , 14% waves from 180° to 225° , and the rest 2% are from 90° to 135° (Mishra et al. 2014). Longshore current patterns of Odisha coast show northerly during March to October, and during November to February, the current moves toward south (Jena et al. 2001). Mishra et al. (2014) has measured the current circulation pattern off Gopalpur and found NE or ENE direction during January to June, while in July, the current changes its direction to ESE. However, net longshore transport direction is toward north. Chandramohan and Nayak (1994) has estimated northerly longshore drift of 1.1×10^6 and $0.51 \times 10^6 \text{ m}^3/\text{year}$ southerly drift.

Materials and methods

Satellite data products of different periods were used for extraction of shoreline, and the detailed information of these images are shown in Table 1. The spatial resolution of the images ranges from 30 m (Landsat) to 2.5 m (Cartosat—I). Landsat data were downloaded from GCLF (<http://gclf.umd.edu/data/>) Web site, and all other data, i.e., LISS-III, LISS-IV and Cartosat are obtained from National Remote Sensing Centre (NRSC), Hyderabad, India. Many researchers (e.g., Maiti and Bhattacharya 2009; Natesan et al. 2014; Shetty et al. 2015) have used published topographical maps for rectifying the satellite images. Using such techniques, it is difficult to select the exact ground control points (GCPs) in both map and satellite images which ultimately affect the accuracy of the shoreline change results. In order to minimize the rectification error, GCPs were collected using handheld trimble geoexplorer global positioning system (Projection type—WGS 1984, geographic). For GCP selection, permanent features such as road intersection, building corner was selected and fixed the GPS error <2 m. Most recent image, i.e., LISS-IV of March 2014 was considered as a master image and used to

register other images. Using field-collected GCPs, master image were rectified by second-order polynomial transformations using Erdas Imagine 2013 software. The number of GCPs used is ranged from 15 to 25, and it is randomly distributed in image. Using image-to-image co-registration method, all other images were rectified and converted into UTM projection for shoreline extraction. In order to check the accuracy of georeferenced images, root mean square error (RMSE) between the GCPs and the geographical coordinates of the same point on georeferenced images were calculated by applying following Eq. (1):

$$\text{RMSE} = \sqrt{\sum_{i=1}^n [(x_s - x_r)^2 + (y_s - y_r)^2]^2} \quad (1)$$

where x_s and y_s are geospatial coordinates of the GCPs collected using GPS; and x_r and y_r are coordinates of the same point on the rectified satellite images. Minimum six points were used for each image for RMSE calculation and total error was maintained below 1 pixel which is approximately 5 m for LISS-IV and Cartosat and 25 m for Landsat and LISS-III images.

Shoreline detection and extraction

An idealized definition of shoreline is that it coincides with the physical interface of land and water (Dolan et al. 1980). There are number of proxies, e.g., dune line (Stafford and Langfelder 1971), bluff top/cliff top (Priest 1999; Guy 1999), vegetation line (Hoeke et al. 2001), high water line (McCurdy 1950; Shalowitz 1964; Dolan et al. 1980; Fenster and Dolan 1999; Zhang et al. 2002), wet/dry line (Overton et al. 1999) were established for shoreline detection and extraction. Among different method, high water line is the most commonly used proxy for shoreline detection. In this research work, wet/dry lines of previous high tide of image acquisition day were manually extracted from all the

Table 1 Description of satellite data used in this study

Satellite	Sensor	Date of image acquisition	Time of image acquisition (GMT + 5.30)	Resolution m	Data source
Landsat	TM	29 November 1990	NA	30	USGS
Landsat	ETM ⁺	13 November 1999	NA	30	USGS
Cartosat	Pan	10 September 2006	05:00:30	2.5	NRSC
Cartosat	Pan	15 April 2006	04:59:20	2.5	NRSC
Cartosat	Pan	18 October 2006	04:54:04	2.5	NRSC
IRS-P6	LISS-III	06 January 2008	05.00.38	23.5	NRSC
IRS-P6	LISS-IV	15 January 2013	05.06.45	5.8	NRSC
IRS-P6	LISS- IV	04 March 2013	05.07.07	5.8	NRSC
IRS-P6	LISS- IV	23 March 2014	05.06.35	5.8	NRSC

images using ArcGIS 10.3 software. Using wet/dry line as shoreline proxy, the error associated with tidal range can be reduced (Kankara et al. 2014, 2015).

Shoreline change analysis

The shoreline change analysis was carried out by using digital shoreline analysis system (DSAS) in GIS environment (Thieler et al. 2009). 3082 transects were generated perpendicular to coastline at 20 m spacing to compute the shoreline change rates considering the spatial resolution of data. The long-term shoreline change rates are calculated for 18, 23, and 24 years covering different periods, i.e., 1990–2008, 1990–2013, and 1990–2014 using WLR method. WLR uses a linear regression taking into account a weight for each shoreline transect according to the shoreline uncertainty and determines a best-fit regression line. The slope of this regression line is the shoreline change rate as in Eq. (2).

$$y = m_w + b_w \tag{2}$$

where m_w is the slope (WLR rate) and b_w is y-intersect (Himmelstoss 2009).

This method is more reliable as it takes into account all available data and captures the nonlinear periodical changes. WLR minimizes potential random error and short-term variability (cyclic changes) through the use of statistical approach (Douglas and Crowell 2000). Along with positional and measurement uncertainties, it gives the standard error of the estimated shoreline change.

Short-term shoreline changes are calculated and analyzed for shorter periods (i.e., <10 years) such as 1990–1999, 1999–2006, 2006–2008, 2008–2013, and 2013–2014 using two data sets, i.e., youngest and oldest to compute the changes for given period. End point rate (EPR) was applied for short-term analysis, as given below:

$$EPR(m/year) = \frac{\text{Distance } (A - B) \text{ in m}}{\text{Time between youngest and oldest shoreline}} \tag{3}$$

The end point rate is found as the difference in shoreline position between the two shoreline years divided by the time between surveys (Hapke et al. 2010). Analysis of short-term shoreline variation will be helpful to study the changes occurred due to seasonal variation and extreme events like cyclone and storm surges. Apart from shoreline change rate analysis, an attempt has been made to quantify the amount of land loss/gain in the study area using geospatial techniques. This is achieved by calculating area between two shorelines for a given period. Figure 2 shows a schematic diagram for the method adopted for land loss/gain estimation.

For detailed analysis, the entire area has been classified into four sectors, i.e., S-I to S-IV (Fig. 1). S-I—start from

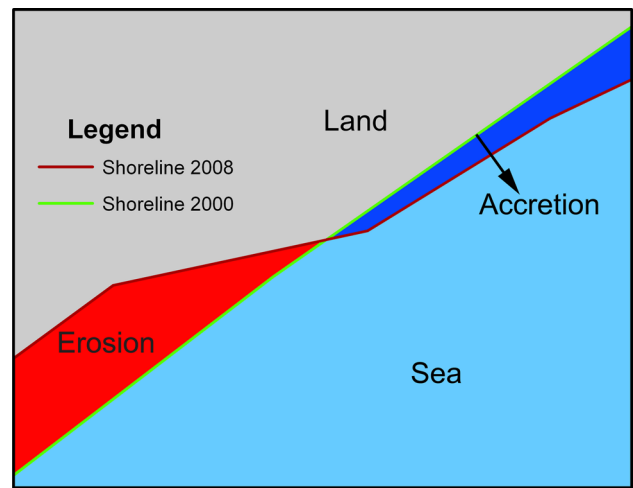


Fig. 2 Schematic diagram showing method adopted for area of land loss/gain calculation

Patisonapur to Markandi river, S-II—Markandi spit to Kharai Nala river, S-III—Kharai Nala river to near Rushikulya river, and S-IV—Rushikulya river to Prayagi. The coastline between two rivers is marked as boundary for each sector which is almost similar to sediment sub-cells.

Results

Long-term changes

Figure 3 shows the long-term (1990–2014) shoreline change rate map of Ganjam district, and shoreline change statistics of all four sectors are summarized in Table 2. The results indicate that major part of the coastline in the districts falls under accretion category. Maximum percentage of erosion was noticed in S-IV (37.92 %) and S-III (32.70 %), whereas S-I and S-II show maximum accretion of 83.52 and 76.80 %, respectively. As mean shoreline change rate is concern, S-I and S-III shows the maximum value of 1.43 and 1.50 m/year, respectively (Table 2). From long-term shoreline change analysis, it is found that Ganjam coast is accreting with a rate of 1.12 m/year between 1990 and 2014.

The cumulative long-term shoreline change rate for 18, 23, and 24 years (1990–2008, 1990–2013 and 1990–2014) are shown in Fig. 4. From Fig. 4, the gradual increase of accretion in southern part of Gopalpur port is clearly observed, whereas ~8 km stretch of northern part of the port exhibit erosion. Also, it is observed that before construction of breakwater and groins low accretion and erosion rate have been observed in both side of Gopalpur port.

In S-I, except river mouth and creek regions all places shows accretion. High erosion rate of –19.84 m/year has

Fig. 3 Map showing erosion—accretion pattern of Ganjam coast derived using WLR method

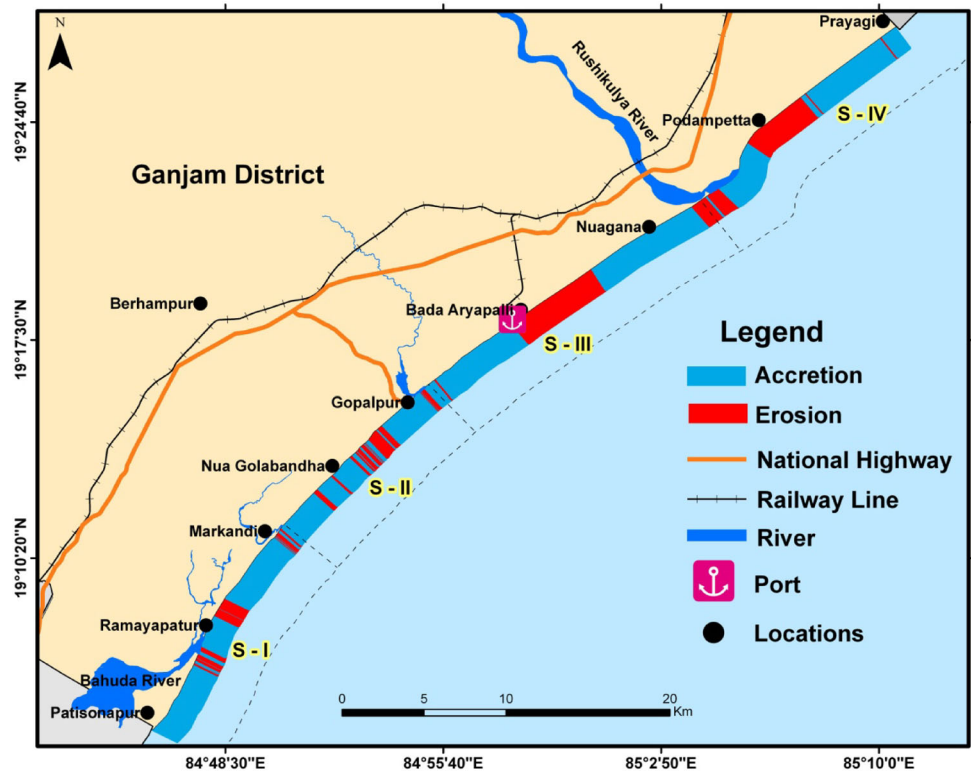


Table 2 Descriptive statistics of long-term (1990–2014) shoreline change rate (m/year) of all four sectors in the study area

Descriptive	S-I	S-II	S-III	S-VI	Total
Mean shoreline change (m/year)	1.43	0.42	1.50	0.97	1.12
Minimum shoreline change (m/year)	-19.84	-1.42	-14.21	-17.31	-19.84
Maximum shoreline change (m/year)	14.60	1.40	19.36	17.09	19.36
Mean accretion rate (m/year)	2.05	0.59	4.61	3.12	2.70
Mean erosion rate (m/year)	-1.70	-0.15	-4.92	-2.53	-2.85
Standard deviation (m/year)	3.01	0.44	6.03	4.90	4.42
Length of shoreline that record erosion (km)	2.40	2.82	5.92	6.34	17.48
Length of shoreline that record accretion (km)	12.16	9.44	12.18	10.38	44.16
% of shoreline subjected to erosion	3.89	4.57	9.60	10.29	28.35
% of shoreline subjected to accretion	19.73	15.31	19.76	16.84	71.65

been observed in Bahuda river mouth. In S-II, erosion is observed in Bauxipalli and Haripur creek areas. All other locations in this sector show accretion with maximum and mean rate of 1.4 and 0.59 m/year, respectively (Table 2). In sector-III, 67.29 % of coastline shows accretion with a mean rate of 4.61 m/year. In this sector, two stretches are found in accretion area: one is ~6 km coastal stretch south of Gopalpur port and other is ~6.1 km of coastline south of Rushikulya river mouth. The most prominent erosion hot spot is northern part of Gopalpur port region where ~5 km of stretch shows erosion. Also this sector shows the maximum standard deviation of 6.03 m/year (Table 2). In S-IV, erosion is mainly found in Rushikulya river mouth and Podampeta–Bateshwar coastal stretch. Major accretion

area of this sector is a 7 km coastal stretch south of Prayagi village. Another accretion area of this sector is located northern side Rushikulya river; here, ~3 km stretch shows accretion.

Short-term changes

Short-term shoreline changes are calculated and analyzed for shorter periods (i.e., <10 years) such as 1990–1999, 1999–2006, 2006–2008, 2008–2013, and 2013–2014 using EPR method, and the sectorwise erosion–accretion patterns are shown in Table 3 and maps are shown in Fig. 5. The detailed description of each sector is as follows.

Fig. 4 Graph showing cumulative shoreline change rate for different periods (1990–2008, 1990–2013, 1990–2014)

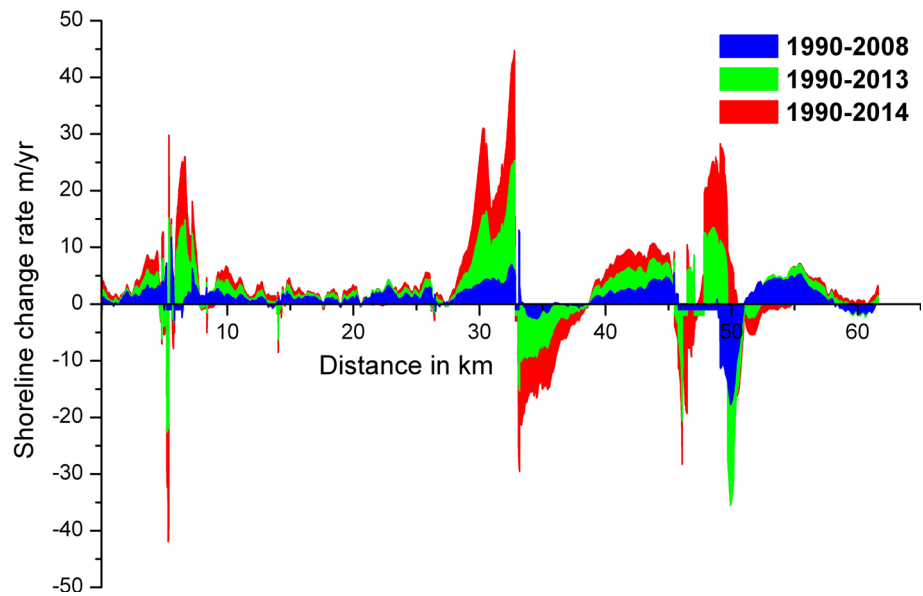


Table 3 Sectorwise shoreline erosion/accretion pattern obtained from EPR analysis of different periods

Sectors	1990–1999		1999–2006		2006–2008		2008–2013		2013–2014	
	Erosion (km)	Accretion (km)	Erosion (km)	Accretion (km)	Erosion (km)	Accretion (km)	Erosion (km)	Accretion (km)	Erosion (km)	Accretion (km)
S-I	7.84	6.72	2.22	12.34	10.78	3.78	5.66	8.90	11.22	3.34
S-II	8.68	3.58	1.42	10.84	10.78	1.48	3.44	8.82	11.86	0.40
S-III	13.58	4.52	0.28	17.82	15.80	2.02	5.46	12.64	8.14	9.96
S-IV	10.66	6.06	7.44	9.28	12.26	4.46	9.46	7.26	12.20	4.52
Total	40.76	20.88	11.36	50.28	49.62	11.74	24.02	37.62	43.42	18.22

Sector-I

This sector consists of 14.56-km-long coastal stretch starting from Patisonapur to Markandi river mouth. It consists of wide beaches with small foreshore sand dunes and three minor river mouths. The backshore area of this sector is mainly covered with plantations. During 1990–1999 period, 7.84 km shoreline exhibit erosion with an average rate of -2.187 m/year (Table 3). Maximum erosion rate (-17.27 m/year) was noticed in the northern part of Bhahuda river spit (Fig. 5a), whereas southern side of the spit shows the accretion pattern. But, in the case of Markandi river, both spits show erosion pattern, whereas ~ 2 km coastline southern side of Markandi river shows accretion. Almost equal amount of land area has been eroded and accreted during this period (Table 4). Comparing shoreline of 1999 and 2006 shows that erosion is reduced during these periods. More than 80 % of shoreline in this sector shows accretion pattern during this period (Fig. 5b). Erosion is observed in spit region of Bhahuda river mouth. Shoreline change rate of this sector range from -10.1 to 24.19 m/year. As

area change is concern, 28.93 ha of land has been accreted during 1999–2006 period (Table 4). Again during 2006–2008 periods, this sector changed into erosion nature (Fig. 5c). About 10.50 km of coastline shows erosion, and accretion was limited only to 3 km stretch in 2006–2008 periods. Accretion was increased during 2008–2013 period with a mean rate of 4.43 m/year. Accretion was observed in ~ 8.9 km coastal stretch and erosion was observed in 5.66 km shoreline in 2008–2013 periods (Fig. 5d). Erosion rate was increased in 2013–2014 periods in which 11.22-km coastline in this sector exhibit erosion (Fig. 5e). Total of 18.33 ha of land has been eroded in this sector during 2013–2014 periods (Table 4).

Sector-II

This stretch is starting from northern end of Markandi spit to Kharai Nala river covering 12.26 km of coastline. There are three fishing villages, and one tourist spot, i.e., Gopalpur beach is located in this stretch. During 1990–1999 periods, more than half of this sector shows

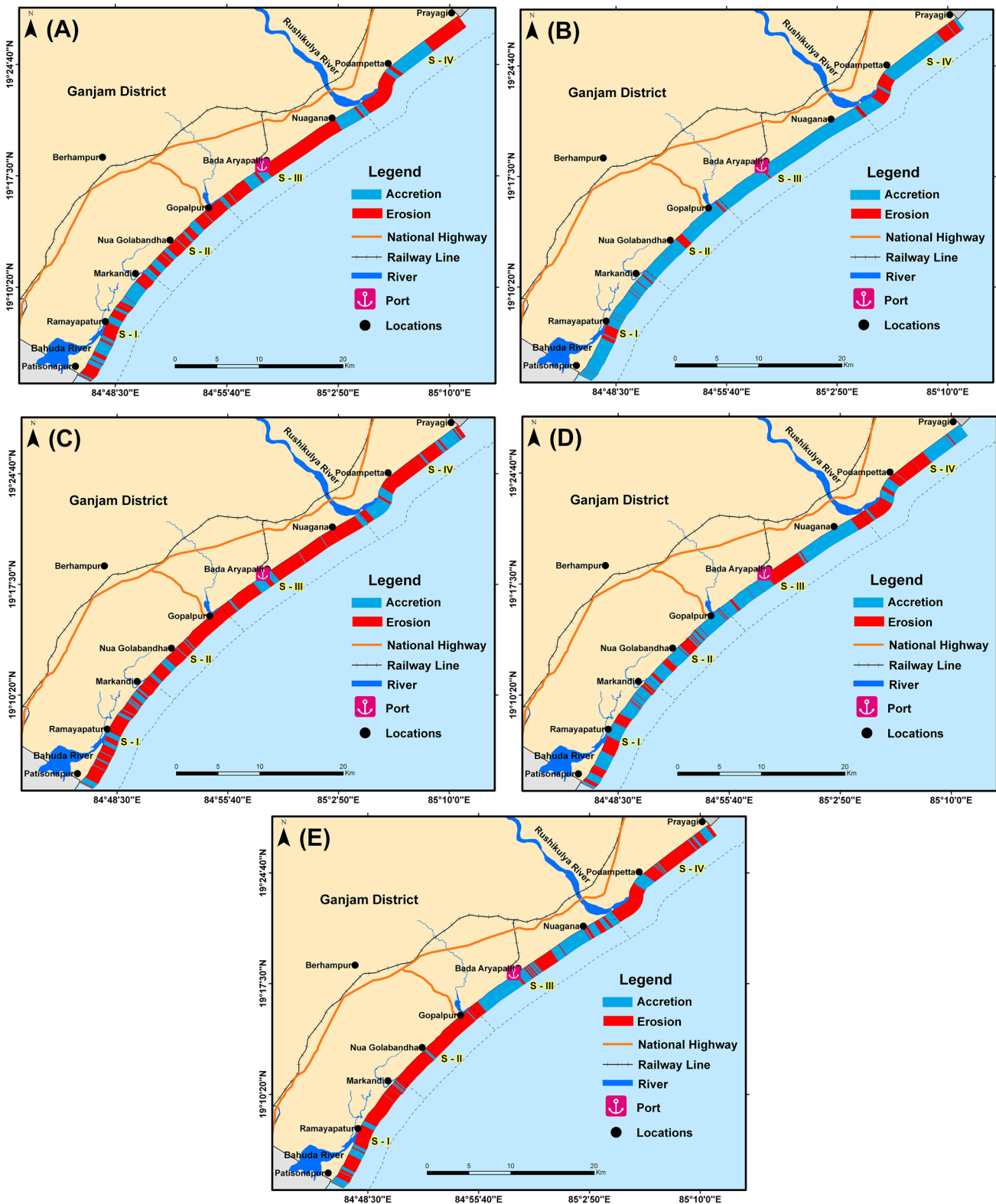


Fig. 5 Maps showing short-term shoreline change rate of different periods. **a** 1990–1999, **b** 1999–2006, **c** 2006–2008, **d** 2008–2013 and **e** 2013–2014 calculated by using EPR method

Table 4 Sectorwise land loss/gain pattern of different periods

Sectors	1990–1999		1999–2006		2006–2008		2008–2013		2013–2014	
	Loss (ha)	Gain (ha)	Loss (ha)	Gain (ha)	Loss (ha)	Gain (ha)	Loss (ha)	Gain (ha)	Loss (ha)	Gain (ha)
S-I	9.55	9.24	4.50	28.93	15.00	4.19	14.57	19.36	18.33	14.64
S-II	9.35	2.41	0.01	27.53	18.40	0.90	2.58	10.45	7.19	1.02
S-III	31.35	7.57	–	66.67	30.31	2.75	31.42	71.23	10.10	16.92
S-IV	60.09	19.25	13.06	25.80	25.47	23.55	13.72	19.95	82.25	14.67
Total	110.34	38.47	17.57	148.93	89.18	31.39	62.29	120.99	117.87	47.25

erosion with a maximum erosion of -7.42 m/year with a mean value of -0.678 m/year, respectively. Maximum accretion rate observed in this stretch is 2.11 m/year. This period witnessed the erosion in Gopalpur and Dhableswar beaches (Fig. 5a). But, during 1999–2006 this sector changed into accretion coast (Fig. 5b). Erosion is limited to only 1.42 km stretch, whereas 10.84 km of shoreline in this sector shows accretion in 1999–2006 period. An area of 27.53 ha was accreted in this sector during 1999–2006 periods. But, during 2006–2008 periods entire shoreline of this sector exhibited erosion with an average rate of -11.65 m/year (Fig. 5c). Erosion is observed in ~ 10.78 km of coastline, and accretion is limited only to 1.48 km during 2006–2008. As area change is concern, 18.40 ha of land was eroded and relatively less area (0.90 ha) was accreted in this sector during 2006–2008 period (Table 4). Accretion was increased to ~ 8.8 km in this sector in 2008–2013 periods, and 3.4 km of coastline shows erosion in this period (Fig. 5d). The entire coastal stretch of this sector shows erosion during 2013–2014 periods with a mean erosion rate of 31.4 m/year (Fig. 5e).

Sector-III

This stretch starts from Kharai Nala river to near Rushikulya river with a coastline length of 18.10 km. The Gopalpur port was found in this stretch. During 1990–1999 period, shoreline change rate of this stretch range from -9.11 to 6.97 m/year, respectively. Out of 18.10 km stretch, 13.58 km of coastline exhibit erosion during 1990–1999 periods. Accretion is found only in a few pockets with a maximum rate of 6.97 m/year. As area change is concern, 31.35 ha of land was eroded and 7.57 ha was accreted in this sector during 1990–1999 period (Table 4). Compared to previous periods (1990–1999), shoreline in this sector shows accretion in 1999–2006 periods (Fig. 5b). The entire coastline in this sector changes in accretion nature with 66.67 ha of accreted area during 1999–2006 periods (Table 4). The coastline in this sector changed into erosion coast during 2006–2008 periods. Erosion was observed in 15.80 km coastline, and 2.3 km shows accretion during this period

(Fig. 5c). Erosion was reduced in this sector during 2008–2013 periods. Accretion was observed in 6 km southern and 7 km northern side of the sector, whereas erosion is found only in ~ 5 km stretch in the central part (Fig. 5d). In both periods, i.e., 2006–2008 and 2008–2013, 30.31 and 31.42 ha of land was eroded in this sector. At the same time, 71.23 ha were accreted during 2008–2013 period (Table 4).

Sector-IV

Sector -IV consists of 16.74 km coastal stretch starting from Rushikulya river to Prayagi light house. Backshore of this stretch consists of medium-sized sand dunes. About 10 km of shoreline exhibits erosion during 1990–1999 periods. High erosion rate (>30 m/year) was observed in Rushikulya river mouth. Accretion was observed only in 6.06 km coastal stretch of Podampetta region (Fig. 5a). Erosion was also noticed in ~ 4 km stretch south of Prayagi light house. As area change is concern, 60.09 ha of land was eroded and 19.25 ha were accreted during 1990–1999 period. Erosion is slightly reduced in this sector during 1999–2006 periods (Fig. 5b). Maximum accretion rate of 9.91 m/year was observed during the same periods. During 2006–2008, 12.26 km of coastline shows erosion and 4.46 km shows accretion in this sector (Fig. 5c). Erosion was slightly reduced in 2008–2013 periods with an average rate of -3.85 m/year. An area of 82.25 ha was eroded during 2013–2014, and 14.66 ha were accreted during the same period (Table 4).

Discussion

The east coast of India is well known for cyclones and storm surges. Frequent occurrence of tropical cyclones and floods plays a major role in shoreline changes in Odisha coast (Mohanty et al. 2008). Figure 6 shows the tracks of depressions and cyclones passed through Odisha coast during the study period (1990–2014). During the month of October 1999, two cyclones hit in Odisha coast within a time span of 2 weeks which affected Ganjam district. A

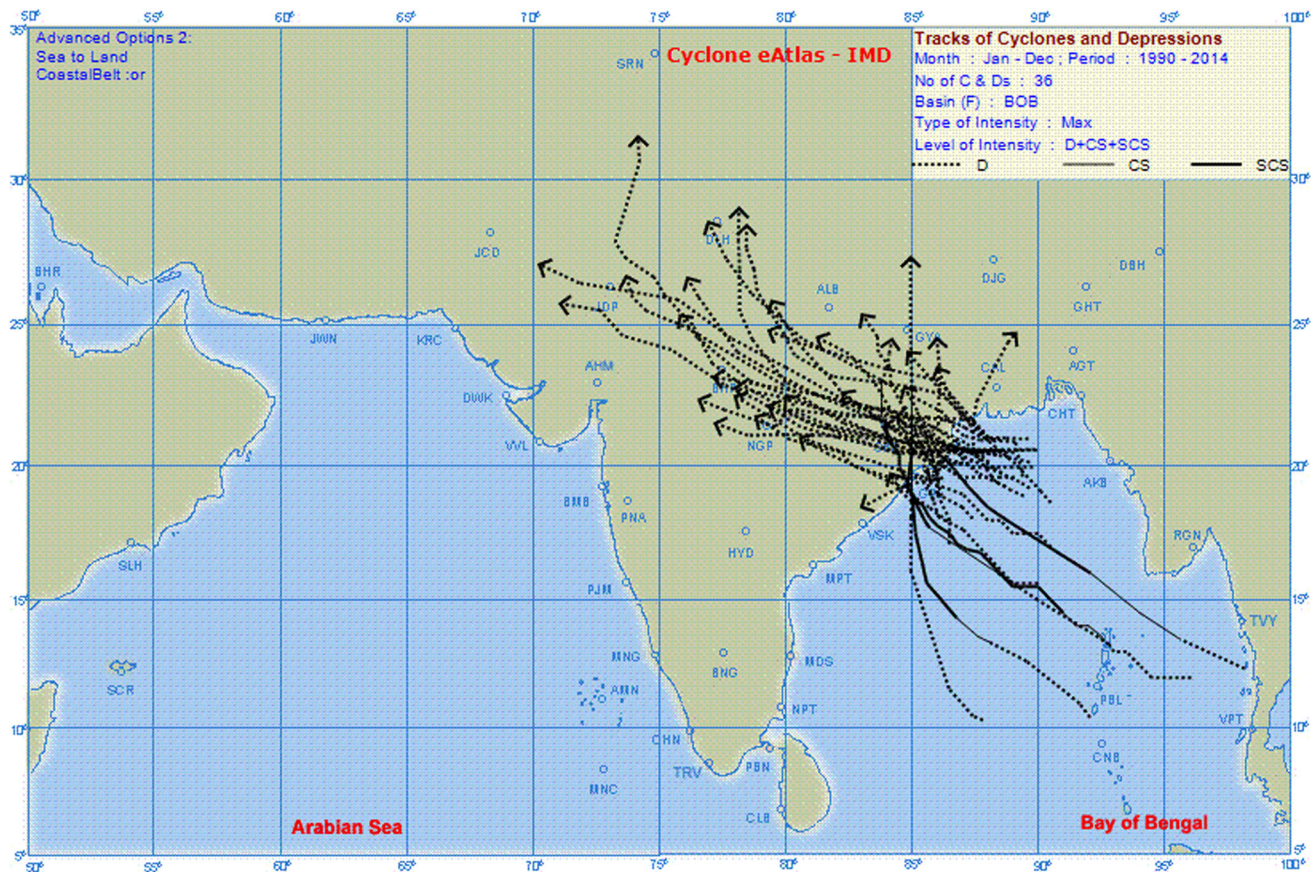


Fig. 6 Map showing tracks of cyclonic storms passed through Odisha coast during study period (1990–2014). Source: Cyclone E-Atlas (IMD 2015)

total of 14 cyclonic events (including depressions) have occurred in Odisha coast during 1991–2000 periods (IMD 2008; Bahinipati 2014). Details of the historical (1905–2013) cyclones that passed through Ganjam and adjacent coast are shown in Table 5. The short-term change results for the period 1990–1999 show high erosion rate in all four sectors in the study area. During 2000–2007 periods, 11 cyclonic events occurred in Odisha coast, and shoreline change rate for the period 1999–2006 shows that all four sectors changed into accretion nature. Recently, two major cyclones Phailin (October 2013) and Hud Hud (October, 2014) hit on east coast of India especially in Odisha and Andhra Pradesh coast. Both were very severe cyclones that occurred after southwest monsoon. Behera et al. (2014) have reported that major part of Ganjam coast has eroded due to due to high waves generated by cyclone Phailin. Amrutha et al. (2014) have observed H_s of 7.3 m off Gopalpur during the Phailin cyclone time, whereas maximum wave height of 8.4 m was observed in Bay of Bengal during 1999 Odisha super cyclone (Rajesh et al. 2005). During Hud Hud cyclone, H_s of 6 m was observed in Gopalpur region (Sirisha et al. 2015). Short-term change

result for the period 2013–2014 shows maximum erosion in all four sectors of Ganjam coast which can be attributed to impact of cyclones. Mishra et al. (2001) have observed that most of the beaches of Ganjam coast are mostly accretional with intermittent erosion during SW monsoon (June to September) period. The long-term shoreline change result of the Ganjam district also confirms this observation. Phailin cyclone was significantly affected in Gopalpur port, where 900 m of southern breakwater was totally devastated. Sundaravadivelu et al. (2015) found that all the groins constructed in the port region were partially damaged due to cyclonic storms.

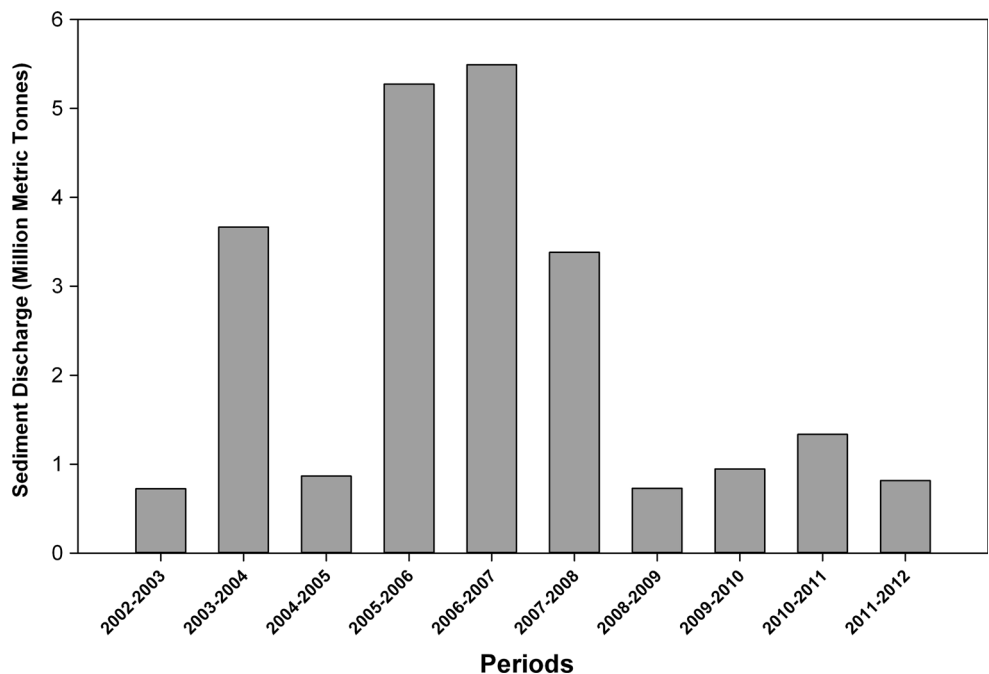
Many studies (e.g., Wells 1996; Kesel 1988; Day et al. 2000) show that reduction in sediment and water discharge from rivers will play a major role in shoreline change pattern especially in deltaic coast. Nineteen dams are constructed across various rivers of Ganjam district mainly for irrigational purposes.¹ These constructions shall have reduced the sediment supply to the sea and which ultimately affect the shoreline configuration. Further study is

¹ http://india-wris.nrsc.gov.in/wrpinfo/index.php?title=Dams_in_Odisha.

Table 5 Details of cyclonic storms that passed through the Ganjam and adjacent coast of Odisha during 1905–2013 (modified from Chittibabu et al. 2004; Mishra and Panigrahi 2014)

Sl. no.	Year and date	Type	Landfall location
1	22nd September, 1905	Cyclonic storm	Between Visakhapatnam and Gopalpur
2	26th October, 1909	Severe cyclonic storm	Gopalpur
3	13th May, 1910	Severe cyclonic storm	Gopalpur
4	13th November, 1923	Very severe cyclonic storm	Gopalpur
5	19th November, 1924	Severe cyclonic storm	Gopalpur
6	04th November, 1936	Very severe cyclonic storm	Puri
7	10th October, 1938	Very severe cyclonic storm	Ganjam
8	16th November, 1942	Very severe cyclonic storm	Ganjam
9	30th October, 1943	Severe cyclonic storm	Chilka
10	19th August, 1957	Severe cyclonic storm	Chilka
11	9th October, 1967	Very severe cyclonic storm	Puri
12	10th September, 1968	Severe cyclonic storm	Chilka
13	26th September, 1968	Severe cyclonic storm	Chilka
14	29th September, 1968	Severe cyclonic storm	Chilka
15	10th November, 1968	Severe cyclonic storm	Chilka
16	7th September, 1971	Very severe cyclonic storm	Chilka
17	22nd September, 1972	Very severe cyclonic storm	Gopalpur
18	24th September, 1981	Severe cyclonic storm	Puri
19	20th September, 1985	Severe cyclonic storm	Puri
20	21st July, 1989	Severe cyclonic storm	Gopalpur
21	7th November, 1995	Very severe cyclonic storm	Gopalpur
22	15th October, 1999	Very severe cyclonic storm	Gopalpur
23	12th October, 2013	Very severe cyclonic storm	Gopalpur

Fig. 7 Graph showing sediment discharge (2002–2012) data of Rushikulya river (data source: CWC 2015)



required to find the impact of these dams in shoreline change patterns.

Rushikulya is a major river in the study area which covers drainage area of 8963 km² with a total length of 160 km.

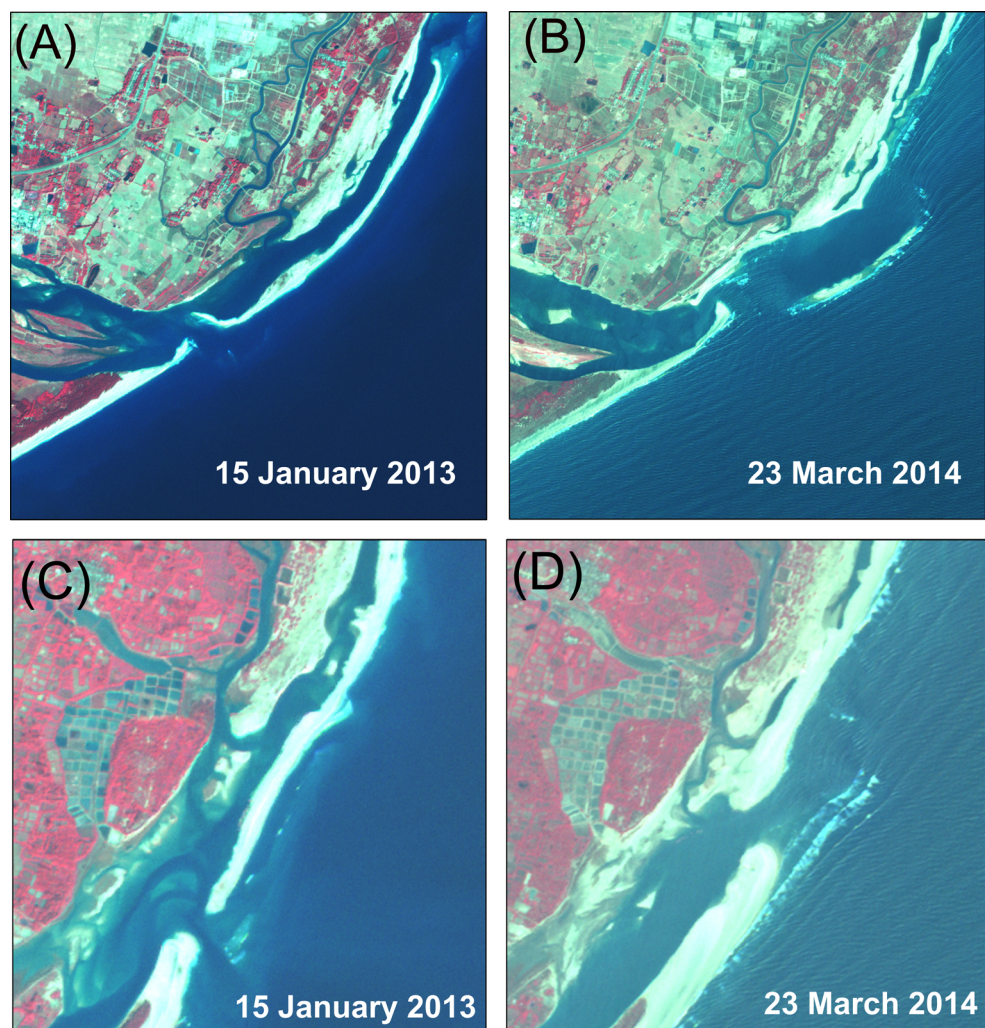
Shoreline change analysis of Rushikulya estuary shows that the region is more dynamic and is changing the river mouth configuration in different periods. Yearly (2002–2012) sediment discharge data of Rushikulya river reveal that

maximum sediment discharge occurred during the period between 2005 and 2007 (Fig. 7). Accretion observed during 1999–2006 period can be attributed to high sediment discharge observed in Rushikulya river during 2005–2007 periods. After 2008, sediment discharge has reduced by more than 50 %. The sand spit formed in the river mouth has also showed accretional trend during 2003–2013 periods, and after Phailin cyclone, length of the sand spit has been reduced (Kumar et al. 2014). Compared with 2013 and 2014 shoreline position, it is found that 750 m of the spit was eroded which is mainly due to Phailin cyclone (Fig. 8a, b). More information of morphodynamics of Rushikulya spit is found in the research work conducted by Pradhan et al. (2015). Apart from Rushikulya river, the spit formed at Bahuda river also shows significant morphological changes after Phailin cyclone. The length of the southern spit of Bahuda river is increased after cyclonic events, whereas northern spit has been eroded (Fig. 8c, d).

The reason for the high erosion rate in S-II is attributed to anthropogenic activity mainly the construction of

Gopalpur port. The port has been constructed in 1987 with one pier, and in 2007, expansion of port is initiated. Two groins 530 m long on southern side and 370 m north on both sides of the channel are constructed during 2007–2010 periods, and 10 groins are constructed in northern side during 2012 (Mishra et al. 2014). Apart from this, 365 m breakwater has constructed in northern side and 1765 m on southern side during 2012–2013 periods (Sundaravadivelu et al. 2015). The present study found that these structures play a major role in shoreline configuration in Ganjam coast. Gopalpur port region falls in sector-III, where shoreline shows maximum erosion especially in northern part of the port and in the southern part it is showing accretion (Fig. 3). During 1990–1999 period, the northern part of the port shows erosion and accretion was limited only to <1 km stretch of southern side. The erosion in this period is mainly due to the impact of super cyclone of 1999. The coastline of Gopalpur port region is again changed into accretion nature during 1999–2006 periods. Again in 2006–2008 periods, the northern part of the port

Fig. 8 Geomorphological changes of spits. **a** Rushikulya spit during 2013, **b** same location at 2014. Note the complete erosion of the spit mainly due to Phailin cyclone. **c** Bahuda spit morphological changes during 2013, **d** same location at 2014. Note the erosion at the northern spit during 2014



changed into erosion and slight accretion was noticed in south side. These changes are mainly due to construction of groins during 2007–2008 periods. The short-term change in 2008–2013 periods clearly shows the complete erosion in northern side of the port up to 4.5 km toward north and accretion in the southern side up ~5 km. From this, it is clear that coastal structures constructed in Gopalpur port are controlling the erosion/accretion pattern. Slight accretion observed in northern part of the port during 2013–2014

periods was mainly due to beach nourishment work started since June 2012. Mohanty et al. (2012) have studied the impact of groins in Gopalpur port by analyzing beach profiles and found that the rate of deposition on the southern side of the port is much faster than the rate of erosion on the north. After analyzing long-term shoreline change rate, this study also found same observation. Study conducted before construction of breakwaters and groins found that beaches in Gopalpur regions shows accretion



Fig. 9 Field photograph showing major locations along Ganjam coast. **a** Highly eroding Aryapalli beach located on the northern side of Gopalpur port, **b** partially collapsed groins in Aryapalli, **c** Gopalpur tourist beach, *arrow* indicate the collapsed buildings due to past

cyclonic events, **d** spit formed in Marakandi river mouth, **e** wide long beach of Patisonapur, showing accretion pattern, **f** Prayagi light house beach with dunes

pattern except SW monsoon period (Mishra et al. 2001). Later studies show the Gopalpur region experiencing erosion, which is mainly due to breakwaters and groins constructions (Patanaik 2004; Sanil Kumar et al. 2006). In order to validate the results, field check has been carried out during the month of December 2014 throughout the study area. During field, shoreline position (wet/dry line) was delineated using GPS and validated with shoreline extracted from image. Also, we collected the information from local fishermen to know the seasonal past shoreline configuration. The fishing villages such as Bada Aryapalli and Sana Aryapalli show high erosion (Fig. 9a, b), whereas Gopalpur tourist beach located in southern side port shows accretion (Fig. 9c). Beaches situated in further south of Gopalpur, e.g., Patisonapur, Marakandi, Ramayapatnam, etc. show accretion (Fig. 9d, e). Prayagi lighthouse beach located at the northern end of the district shows stable condition with foreshore dunes (Fig. 9f).

Like all other parts of the world, shoreline changes in the Ganjam coast are mainly due to natural and anthropogenic activities. Natural factors include repeated cyclonic events, high wave height, and wave periods during SW monsoon. Anthropogenic factors such as port development, breakwater, and groin construction are the major causes for shoreline change pattern.

Accuracy of any shoreline change study depends on various factors such as resolution of the satellite sensor, accurate delineation of shoreline, tidal range variation, and image rectification error. The current research work was limited to understand annual-to-decadal shoreline changes using satellite data of different years. Spatial resolution of the sensor is a deciding factor to estimate the periodical shoreline changes. Medium-resolution satellite sensors Landsat TM, IRS-LISS-III, etc. cause mixed pixel problem for shoreline delineation, while high-resolution sensors like LISS-IV are suitable to capture annual changes (Lu et al. 2011). In this study, in three periods (i.e., 2006, 2013 and 2014) high-resolution data were used for shoreline extraction so that the mixed pixel problem was reduced in this study to estimate interdecadal changes.

Region-specific shoreline change analysis is an essential component for developing a shoreline management plan. This is the first shoreline change study carried out in Odisha coast using combination of medium- and high-resolution satellite images, and it provides detailed information on shoreline changes with field verification of results. This research work standardizes the methodology to monitor the shoreline changes using different resolution data sets in a microtidal environment. The analysis reveals that shoreline of Ganjam coast is affected by several cyclones/storm every year. Further, the construction of breakwater and groins obstruct the free flow of sediment along the coast which results accumulation of sand in updrift side and erosion along

downdraft coast. The beach nourishment carried out between groins as a shoreline management plan of Gopalpur port to minimize the erosion has not yielded expected results as it was washed away due to Phailin cyclone. For controlling coastal erosion along Ganjam coast, a comprehensive shoreline management plan is needed within the frame work of Integrated Coastal Zone Management (ICZM). It is recommended that proper Environmental Impact Assessment (EIA) studies need to be carried out using site-specific near-shore hydrodynamic and sediment budget studies before giving approval for coastal establishment such as ports and harbors.

Conclusion

Understanding of shoreline changes on seasonal, annual, short- and long-term provides a foundation to develop a sustainable shoreline management plan. Shoreline change rate analysis of Ganjam coast has been studied in order to identify the erosion accretion pattern. Shoreline of different period was extracted from various satellite images acquired in different years. Long-term shoreline change rate has been carried out for the period 1990–2014 using WLR method. Short-term change analysis was carried out for five period—1990–1999, 1999–2006, 2006–2008, 2008–2013, and 2013–2014—using EPR method. Long-term shoreline change rate results reveal that 71.65 % of the coast falls under accretion and 28.35 % coast falls under erosion categories. From short-term change analysis, the cyclic nature of erosion/accretion pattern is found. Maximum erosion (49.62 km) was observed during 2006–2008 period followed by 42.43 km during 2013–2014. Short-term change for the period 1999–2006 has been noticed as maximum accretion period. Maximum land loss of 110.34 ha was noticed during 1990–1999 and minimum of 17.57 ha were observed in 1999–2006. As the causes of shoreline change are concern, frequent occurrence of tropical cyclones and anthropogenic activities such port development, breakwater and groin constructions are the major factors responsible for shoreline change of Ganjam coast. After construction of breakwaters and groins, northern part of Gopalpur port is continuously eroding, whereas in southern side it shows accretion. This is mainly because of the interception of longshore drift by breakwater and groins. The beach nourishment work carried out since 2012 did not reduced the erosion in northern part of the port. The Phailin cyclone occurred during 2013 significantly damaged the Ganjam coast especially in Gopalpur port region. Due to cyclone, significant morphological changes have been occurred in Rushikulya and Bahuda river mouth. The study proved that the use of multiresolution satellite images has to be an effective approach for estimating shoreline change rate in microtidal region.

Acknowledgments Authors would like to thank Secretary, Ministry of Earth Sciences, Government of India and Project Director ICMAM, for their keen interest and encouragement for this work. The authors are thankful to all the anonymous reviewers for giving valuable suggestions which improve the quality of the manuscript.

References

- Aiello A, Canora F, Pasquariello G, Spilatro G (2013) Shoreline variations and coastal dynamics: a space time data analysis of the Jonian littoral, Italy. *Estuar Coast Shelf Sci* 129:124–135
- Albert P, Jorge G (1998) Coastal changes in the Ebro delta: natural and human factors. *J Coast Conserv* 4:17–26
- Amrutha MM, Sanil Kumar V, Anoop TR, Nair TMB, Nherakkol A, Jeyakumar C (2014) Waves off Gopalpur, northern Bay of Bengal during Cyclone Phailin. *Ann Geophys* 32:1073–1083
- Anderson TR, Frazer LN, Fletcher CH (2015) Long-term Shoreline change at Kailua, Hawaii, using regularized single transect. *J Coast Res* 31(20):464–476
- Bahinipati CS (2014) Assessment of vulnerability to cyclones and floods in Odisha, India: a district-level analysis. *Curr Sci* 107(12):1997–2007
- Bastos L, Bio A, Pinho JLS, Granja H, da Silva AJ (2012) Dynamics of the Douro estuary sand spit before and after breakwater construction. *Estuar Coast Shelf Sci* 109:53–69
- Behera SK, Mohanta RK, Kar C, Mishra SS (2014) Impacts of the super cyclone Philine on sea turtle nesting habitats at the Rushikulya Rookery, Ganjam Coast, India. *Poult Fish Wildl Sci* 2:1–5. doi:10.4172/2375-446X.1000114
- Central Water Commission (2015) Integrated hydrological data book (non-classified river basins). Hydrological data directorate Information Systems Organization, Water planning and projects wing, Central water commission, New Delhi, p 298
- Chandramohan P, Nayak BU (1994) A study for the improvement of Chilka lake tidal inlet, east coast of India. *J Coast Res* 10:909–918
- Chandramohan P, Sanil Kumar V, Nayak BU (1993) Coastal processes along the shorefront of Chilka lake, east coast of India. *Ind J Mar Sci* 22:268–272
- Chittibabu P, Dube SK, Macnabb JB, Murty TS, Rao AD, Mohanty UC, Sinha P (2004) Mitigation of flooding and cyclone hazard in Orissa, India. *Nat Haz* 31:455–485
- Chu ZX, Sun XG, Zhai SK, Xu KH (2006) Changing pattern of accretion/erosion of the modern Yellow river (Huanghe) sub-aerial delta, China, Based on remote sensing images. *Mar Geol* 227(1–2):13–30
- Day JW Jr, Britsch LD, Hawes SR, Shaffer GP, Reed DJ, Cahoon D (2000) Pattern and process of land loss in the Mississippi delta: a spatial and temporal analysis of wetland habitat change. *Estuaries* 23:425–438
- Dolan R, Hayden BP, May P, May SK (1980) The reliability of shoreline change measurements from aerial photographs. *Shore Beach* 48(4):22–29
- Dolan R, Fenster MS, Stuart JH (1991) Temporal analysis of shoreline recession and accretion. *J Coast Res* 7:723–744
- Douglas BC, Crowell M (2000) Long-term shoreline position prediction and error propagation. *J Coast Res* 16:145–152
- El Banna MM, Hereher ME (2009) Detecting temporal shoreline changes and erosion/accretion rates, using remote sensing, and their associated sediment characteristics along the coast of North Sinai, Egypt. *Environ Geol* 58(7):1419–1427
- Fenster MS, Dolan R (1999) Mapping erosion hazard areas in the city of Virginia Beach. *J Coast Res* 28:56–68
- Ford M (2013) Shoreline changes interpreted from multi-temporal aerial photographs and high resolution satellite images: Wotje Atoll, Marshall Islands. *Remote Sens Environ* 135:130–140
- Frihy OE, Dewidar KM (2003) Patterns of erosion/sedimentation, heavy mineral concentration and grain size to interpret boundaries of littoral sub-cells of the Nile delta, Egypt. *Mar Geol* 199:27–43
- Giosan L, Constantinescu S, Clift PD, Tabrez AR, Danish M, Inam A (2006) Recent morphodynamics of the Indus delta shelf and coast. *Cont Shelf Res* 26:1668–1684
- Gonçalves RM, Awange J, Krueger CP, Heck B, Coelho LA (2012) Comparison between three short-term shoreline prediction models. *Ocean Coast Manage* 69:102–110
- Guneroglu A (2015) Coastal changes and land use alteration on Northeastern part of Turkey. *Ocean Coast Manage* 118:225–233
- Guy DE (1999) Erosion hazard area mapping, Lake county, Ohio. *J Coast Res* 28:185–196
- Hanangond PT, Mitra D (2007) Dynamics of the Karwar coast, India, with special reference to study of tectonics and coastal evolution using remote sensing. *J Coast Res* 50:842–847
- Hapke CJ, Himmelstoss EA, Kratzmann M, List JH, Thieler ER (2010) National assessment of shoreline change: historical shoreline change along the New England and Mid-Atlantic coasts: U.S. geological survey open file report 2010–1118, p 57
- Himmelstoss EA (2009) DSAS 4.0 Installation instructions and user guide. In: Thieler ER, Himmelstoss EA, Zichichi JL, Ergul, Ayhan (2009) Digital shoreline analysis system (DSAS) version 4.0—an ArcGIS extension for calculating shoreline change: U.S. geological survey open-file report 2008–1278. *updated for version 4.3, p 79
- Hoeke RK, Zarillo GA, Synder M (2001) A GIS based tool for extracting shoreline positions from aerial imagery (BEACH-TOOLS). US Army Corps of Engineers, Coastal Engineering Technical Note IV, Washington, DC, p 12
- Houser C, Hapke C, Hamilton S (2008) Controls on coastal dune morphology, shoreline erosion and barrier island response to extreme storms. *Geomorphology* 100:223–240
- India Meteorological Department (IMD) (2008) Electronic atlas of tracks of cyclones and depressions in the Bay of Bengal and the Arabian Sea, version 1.0/2008” CD Rom, India Meteorological Department, Chennai
- India Meteorological Department (IMD) (2015) Cyclone eAtlas-IMD-tracks of cyclones and depressions over North Indian Ocean 1891–2014, version 2.0/2011, Regional Meteorological Centre, Chennai
- Jayappa KS, Vijaya Kumar GT, Subrahmanya KR (2003) Influence of coastal structures on beach morphology and shoreline in southern Karnataka, India. *J Coast Res* 68:874–884
- Jena BK, Chandramohan P, Sanil Kumar V (2001) Longshore transport based on directional waves along north Tamil Nadu Coast, India. *J Coast Res* 17:322–327
- Jimenez JA, Sanchez-Arcilla A, Valdemoro HI, Gracia V, Nieto F (1997) Processes reshaping the Ebro delta. *Mar Geol* 144:59–79
- Kaliraj S, Chandrasekar N, Magesh NS (2013) Impacts of wave energy and littoral currents on shoreline erosion/accretion along the south-west coast of Kanyakumari, Tamil Nadu using DSAS and geospatial technology. *Environ Earth Sci* 71(10):4523–4542
- Kaliraj S, Chandrasekar N, Magesh NS (2015) Evaluation of coastal erosion and accretion processes along the southwest coast of Kanyakumari, Tamil Nadu using geospatial techniques. *Arab J Geosci* 8(1):239–253
- Kankara RS, Selvan CS, Rajan B, Arockiaraj S (2014) An adaptive approach to monitor the shoreline changes in ICZM framework: a case study of Chennai coast. *Ind J Mar Sci* 43(7):1271–1279
- Kankara RS, Selvan SC, Markose VJ, Rajan B, Arockiaraj S (2015) Estimation of long and short term shoreline changes along

- Andhra Pradesh coast using remote sensing and GIS techniques. *Procedia Eng* 116:855–862
- Kesel RH (1988) The decline of the suspended load of the lower Mississippi river and its influence on adjacent wetlands. *Environ Geol Water Sci* 11:271–281
- Kim IH, Lee HS, Kim JH, Yoon JS, Hur DS (2014) Shoreline change due to construction of the artificial headland with submerged breakwaters. *J Coast Res* 72:145–150
- Kuleli T, Guneroglu A, Karsli F, Dihkan M (2011) Automatic detection of shoreline change on coastal Ramsar wetlands of Turkey. *Ocean Eng* 38:1141–1149
- Kumar HS, Panditrao S, Baliarsingh SK, Mohanty P, Mahendra RS, Lotliker AA, Kumar TS (2014) Consequence of cyclonic storm Phailin on coastal morphology of Rushikulya estuary: an arribada site of vulnerable Olive Ridley sea turtles along the east coast of India. *Curr Sci* 107(1):28–30
- Li X, Zhou Y, Zhang L, Kuang R (2014) Shoreline change of Chongming Dongtan and response to river sediment load: a remote sensing assessment. *J Hydrol* 511:432–442
- Lu D, Moran E, Hetrick S, Li G (2011) Mapping impervious surface distribution with the integration of Landsat TM and QuickBird images in a complex urban–rural frontier in Brazil. In: Chang NB (ed) *Advances of environmental remote sensing to monitor global changes*. CRC Press/Taylor and Francis, Boca Raton, pp 277–296
- Luecke DF, Pitt J, Congdon C, Glenn E, Valdes-Casillas C, Briggs M (1999) A delta once more: restoring riparian and wetland habitat in the Colorado river delta. Environmental Defense Publications, D.C. p 51
- Maiti S, Bhattacharya AK (2009) Shoreline change analysis and its application to prediction: a remote sensing and statistics based approach. *Mar Geol* 257:11–23
- Malini BH, Rao KN (2004) Coastal erosion and habitat loss along the Godavari delta front—a fallout of dam construction. *Curr Sci* 87:1232–1236
- Manca E, Pascucci V, Deluca M, Cossu A, Andreucci S (2013) Shoreline evolution related to coastal development of a managed beach in Alghero, Sardinia, Italy. *Ocean Coast Manage* 85:65–76
- Mani Murali R, Shrivastava D, Vethamony P (2009) Monitoring shoreline environment of Paradip, east coast of India using remote sensing. *Curr Sci* 97(1):79–84
- Mani Murali R, Dhiman R, Choudhary R, Seelam JK, Ilangovan D, Vethamony P (2015) Decadal shoreline assessment using remote sensing along the central Odisha coast, India. *Environ Earth Sci* 74(10):7201–7213
- Mccurdy PG (1950) Coastal delineation from aerial photographs. *Photogramm Eng* 16(4):550–555
- Mishra SP, Panigrahi R (2014) Storm impact on south Odisha coast, India. *Int J Adv Res Sci Eng* 11(3):209–225
- Mishra P, Mohanty PK, Murty ASN, Sugimoto T (2001) Beach profile studies near an artificial open coast port along South Orissa. East coast of coast of India. *J Coast Res* 34:164–171
- Mishra P, Patra SK, Ramana Murthy MV, Mohanty PK, Panda US (2011) Interaction of monsoonal wave, current and tide near Gopalpur, east coast of India, and their impact on beach profile: a case study. *Nat Haz* 59:1145–1159
- Mishra P, Pradhan UK, Panda US, Patra SK, Ramana Murthy MV, Seth B, Mohanty PK (2014) Field measurements and numerical modelling of nearshore processes at an open coast port on the east coast of India of India. *Ind J Geo-Mar Sci* 43:1277–1285
- Mohanty PK, Panda US, Pal SR, Mishra P (2008) Monitoring and management of environmental changes along the Orissa coast. *J Coast Res* 24(2B):13–27
- Mohanty PK, Patra SK, Bramha S, Seth B, Pradhan UK, Behera B, Mishra P, Panda US (2012) Impact of groins on beach morphology: a case study near Gopalpur port, east coast of India. *J Coast Res* 28(1):132–142
- Mohanty PK, Barik SK, Kar PK, Behera B, Mishra P (2015) Impacts of ports onshoreline change along Odisha coast. *Procedia Eng* 116:647–654
- Morton RA, Miller TL (2005) National assessment of shoreline change: part 2: historical shoreline change and associated land loss along the U.S. south east Atlantic Coast: U.S. geological survey open-file report 2005–1401
- Natesan U, Thulasiraman N, Deepthi K, Kathiravan K (2013) Shoreline change analysis of Vedaranyam coast, Tamil Nadu, India. *Environ Monit Assess* 185(6):5099–5109
- Natesan U, Rajalakshmi PR, Ferrer VA (2014) Shoreline dynamics and littoral transport around the tidal inlet at Pulicat, southeast coast of India. *Cont Shelf Res* 80:49–56
- Overton MF, Grenier RR, Judge EK, Fisher JS (1999) Identification and analysis of coastal erosion hazard areas: Dare and Brunswick Counties, north Carolina. *J Coast Res* 28:69–84
- Ozturk D, Sesli FA (2015) Shoreline change analysis of the Kizilirmak Lagoon series. *Ocean Coast Manage* 118:290–308
- Ozturk D, Beyazit I, Kilic F (2015) Spatiotemporal analysis of shoreline changes of the Kizilirmak delta. *J Coast Res* 31(6):1389–1402
- Patanaik SK (2004) Coastal processes near Gopalpur port, east coast of India. M.Phil thesis, Berhampur University, India, pp 34–36
- Pradhan U, Mishra P, Mohanty PK, Behera B (2015) Formation, growth and variability of sand spit at Rushikulya river mouth, south Odisha coast, India. *Procedia Eng* 116:963–970
- Priest GR (1999) Coastal shoreline change study: northern and central Lincoln county, Oregon. *J Coast Res* 28:140–157
- Rajawat AS, Chauhan HB, Ratheesh R, Rhode S, Bhandari RJ, Mahapatra M, Kumar M, Yadav R, Abraham SP, Singh SS, Keshri KN, Ajai (2015) Assessment of coastal erosion along the Indian coast on 1:25,000 scale using satellite data of 1989–1991 and 2004–2006 time frames. *Curr Sci* 109(2):347–353
- Rajesh G, Jossia Joseph K, Hari Krishnan M, Premkumar K (2005) Observations on extreme meteorological and oceanographic parameters in Indian seas. *Curr Sci* 88:1279–1282
- Ramana Murthy MV, Mani JS, Subramanian BR (2007) Evolution and performance of beachfill at Ennore seaport, south east coast of India. *J Coast Res* 24(1A):232–243
- Ranga Rao V, Ramana Murthy MV, Bhat M, Reddy NT (2009) Littoral sediment transport and shoreline changes along Ennore on the south east coast of India: field observations and numerical modeling. *Geomorphology* 112:158–166
- Rao KN, Subraelu P, Kumar KChV, Demudu G, Malini BH, Rajawat AS, Ajai (2010) Impacts of sediment retention by dams on delta shoreline recession: evidences from the Krishna and Godavari deltas, India. *Earth Surf Proc Land* 35:817–827
- Samsuddin M, Suchindan GK (1987) Beach erosion and accretion in relation to seasonal longshore current variation in the northern Kerala coast, India. *J Coast Res* 3(1):55–62
- Sanil Kumar V, Pathak KC, Pednekar P, Raju NSN, Gowthaman R (2006) Coastal processes along the Indian coastline. *Curr Sci* 91:530–536
- Selvan SC, Kankara RS, Markose VJ, Rajan B, Prabhu K (2016) Shoreline change and impacts of coastal protection structures on Puducherry, SE coast of India. *Nat Haz*. doi:10.1007/s11069-016-2332-y
- Shalowitz AL (1964) Shore and sea boundaries with special reference to the interpretation and use of coast and geodetic survey data (publication 10-1). US Government Printing Office, US Department of Commerce, Coast and Geodetic Survey, Washington, DC, p 484
- Shetty A, Jayappaa KS, Mitra D (2015) Shoreline change analysis of Mangalore coast and morphometric analysis of Netravathi–Gurupur and Mulky–Pavanje spits. *Aquat Procedia* 4:182–189

- Shtienberg G, Zviely D, Sivan D, Lazar M (2014) Two centuries of coastal change at Caesarea, Israel: natural processes vs. human intervention. *Geo-Mar Lett* 34:365–379
- Sirisha P, Remya PG, Nair TMB, Venkateswara Rao B (2015) Numerical simulation and observations of very severe cyclone generated surface wave fields in the north Indian Ocean. *J Earth Syst Sci* 124:1639–1651
- Sridhar RS, Elangovan K, Suresh PK (2009) Long term shoreline oscillation and changes of Cauvery delta coastline inferred from satellite imageries. *J Indian Soc Remote Sens* 37(1):79–88
- Stafford DB, Langfelder J (1971) Air photo survey of coastal erosion. *Photogramm Eng* 37(6):565–575
- Sundaravadivelu R, Sakthivel S, Panigrahi PK, Sannasiraj SA (2015) Post-Phailin restoration of Gopalpur port. *Aquat Procedia* 4:365–372
- Syvitski JPM, Saito Y (2007) Morphodynamics of deltas under the influence of humans. *Glob Planet Change* 57:261–282
- Thanh TD, Saito Y, Huy DV, Nguyen VL, Ta TKO, Tateishi M (2004) Regimes of human and climate impacts on coastal changes in Vietnam. *Reg Environ Change* 4:49–62
- Thieler ER, Himmelstoss EA, Zichichi JL, Ergul A (2009) Digital shoreline analysis system (DSAS) version 4.0—an ArcGIS extension for calculating shoreline change: U.S. geological survey open-file report 2008–1278
- Thiruvankatasamy K, Girija DKB (2014) Shoreline evolution due to construction of rubble mound jetties at Munambam inlet in Ernakulam–Trichur district of the state of Kerala in the Indian peninsula. *Ocean Coast Manage* 102:234–247
- Wells JT (1996) Subsidence, sea-level rise, and wetland loss in the lower Mississippi river delta. In: Milliman JD, Haq BU (eds) *Sea-level rise and coastal subsidence*. Kluwer Academic Publishers, Amsterdam, pp 281–311
- Zhang K, Huang W, Douglas BC, Leatherman SP (2002) Shoreline position variability and long-term trend analysis. *Shore Beach* 70(2):31–35
- Zviely D, Kit E, Rosen B, Galili E, Klein M (2009) Shoreline migration and beach-near shore sand balance over the last 200 years in Haifa Bay (SE Mediterranean). *Geo-Mar Lett* 29:93–110